

CONVECTIVELY-INDUCED PV AND VORTEX ROSSBY WAVES IN HURRICANES RITA AND KATRINA (2005)

Falko Judt and Shuyi S. Chen
Rosenstiel School of Marine and Atmospheric Science, University of Miami
Miami, Florida

1. INTRODUCTION

Radar observations in hurricanes reveal spiraling rainbands emanating from the eyewall and propagating outward in the inner region. Theoretical analysis indicates that these inner bands are azimuthally and radially propagating vortex Rossby waves (VRW) (Montgomery and Kallenbach, 1997). It has been hypothesized that outward propagating VRW redistribute potential vorticity (PV) and momentum within the inner core of a hurricane and may lead to formation of concentric eyewalls through interaction with a secondary ring of PV. However, the lack of simultaneous observations of the inner-core and rainband region makes it difficult to understand the complex interaction. The importance of VRW on hurricane intensity changes remains to be an open question of which this study aims to address using high-resolution model forecasts of Hurricanes Katrina and Rita from the Hurricane Rainbands and Intensity Change Experiment (RAINEX) in 2005. The two major hurricanes went through a similar rapid intensification over the Gulf of Mexico. Both the RAINEX observations and model forecast fields showed that Rita developed a secondary eyewall and went through an eyewall replacement before landfall, whereas Katrina did not. The rainbands, PV distribution and wave properties differ significantly in the two storms. In this study we compare the evolution of the convectively-induced PV and wave activities in Katrina and Rita and examine the interactions between the inner core and rainband regions. A PV budget analysis is conducted to quantify the PV sources and sinks in the inner core and outer regions of the hurricanes. Further examination of eddy momentum flux divergence sheds some

lights on the wave-mean flow interactions from a momentum perspective.

2. MODEL DESCRIPTION

This study uses the model forecast fields from the 5th generation PSU-NCAR non-hydrostatic mesoscale model (MM5) with multi-nested, vortex-following grids of 15, 5, and 1.67 km resolutions, respectively. The model initial and lateral boundary conditions are from the real-time GFDL and NOGAPS model forecast fields. The MM5 forecasts from 0000 UTC on 27-30 August for Katrina and 0000 UTC on 20-25 September for Rita were used in the analysis.

3. PV AND VRW ANALYSES

In Katrina, VRW are generated in the eyewall region and propagate outward smoothly over a relatively long distance. No VRW activity is detectable beyond 80-100 km radius because of the fading PV gradient that cannot support VRW at greater radii. This result indicates that interactions between the VRW and an outer PV anomaly which was absent in Katrina must take place within this region. In contrast, Rita had a secondary ring of enhanced PV, evidently associated with the diabatic heating in the outer rainband region at a radius > 100 km. The analysis shows that between the eyewall and this outer ring of PV, VRW activity is barely detectable in the early stage. This indicates that the enhanced PV in the rainband region was generated independently of VRW. A secondary wind maximum coinciding with the PV maximum is observed in the model output as well as in the airborne measurements. The secondary PV and wind maxima contracted inward with time and eventually become the new eyewall. Only when the developing secondary eyewall gets close to the primary eyewall, VRW are detected in the model output.

Corresponding author address: Falko Judt,
Division of Meteorology and Physical
Oceanography, RSMAS, University of Miami,
Miami, FL
Email: fjudt@rsmas.miami.edu

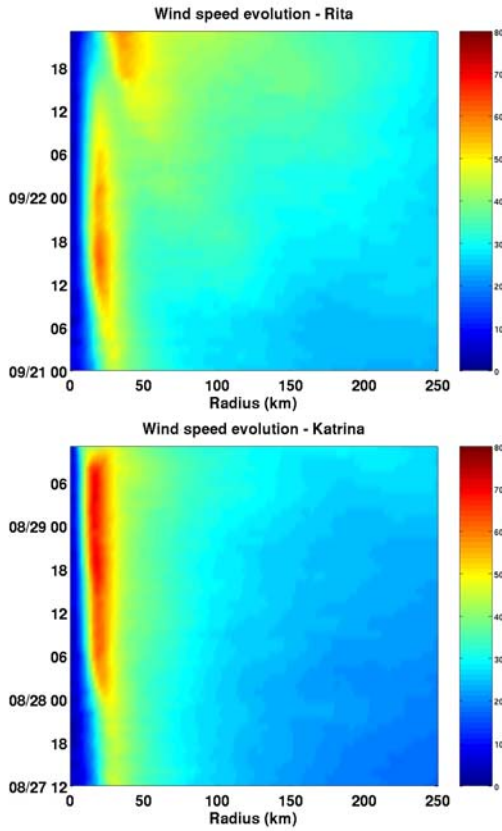


Fig. 1. Wind speed evolution in m s^{-1} of Rita and Katrina. Time in UTC.

The evolution of the azimuthally averaged wind speed at 700 mb shows a secondary wind maximum in Rita which subsequently formed into the secondary eyewall between 06 and 18 UTC SEP 22 (Fig. 1). This feature was, at least in an azimuthally averaged sense, absent in Katrina although the storm featured a secondary vertical velocity peak related to transient rainbands at radii between 40 and 60 km (not shown). In order to conduct a VRW analysis, field variables were Fourier-decomposed into their respective wavenumber components and plotted on a radius-time domain. Previous studies (e.g. Wang, 2002) showed that wave-like features emanating from the eyewall of numerically simulated hurricanes are unambiguously vortex Rossby waves. Figure 2 displays both stationary VRW circling around the RMW (cf. Schubert et al, 1999) as well as outward propagating waves. Field variables in the figures are wavenumber 2 components of rain rate and PV. The gap region between the VRW orbiting the radius of maximum winds (RMW) and the outward propagating waves is due to very strong differential rotation outside

the RMW, any disturbance encountering this area of high shear vanishes quickly by virtue of the axisymmetrization process.

In Rita, non-stationary wave activity is generally absent during the first stage (09 UTC SEP 21 – 03 UTC SEP 22). At this time the secondary wind maximum has already appeared and becomes stronger while it is slowly contracting. Lack of VRW in Rita is probably due to a radial PV profile that does not support radially propagating waves. Comparison of the radial PV gradient between Rita and Katrina indicates a more abrupt decrease in PV in Rita, furthermore the reversal of the PV gradient in Rita does not promote radially outward propagating VRW. A second reason might be a convective unfavorable environment in Rita (descending motion due to the combined outflow of the primary eyewall and the concentric secondary ring of convection) which suppresses the convectively coupled VRW. However, VRW activity begins in Rita once the secondary maximum gets close to the primary eyewall (after 03 UTC SEP 22) when the PV gradient becomes monotonic negative. Katrina's eyewall constantly sheds propagating VRW over the whole time period analyzed.

Montgomery and Kallenbach (1997) proposed a stagnation radius beyond which the waves are not able to propagate. This radius is clearly visible in both cases. In Katrina it is located at 60-80 km and fairly constant in time. In Rita, the stagnation radius decreases from 100 km to 70 km later in the period. According to the original theory, VRW convey and accumulate momentum near the stagnation radius which leads to a secondary wind maximum. The change in wind speed can be determined quantitatively by eddy momentum flux divergence analysis which will be discussed later.

4. PV BUDGET

Following Wang (2002), the PV tendency equation can be written in the form of the Reynolds-decomposition, so that azimuthal averages (mean) and eddy (perturbation) components are obtained. In this study we focused on the tendency of mean PV since the mean state PV evolution determines the structure and intensity of the cyclone on the vortex scale. PV tendency is given by

$$(1) \frac{\partial \bar{P}}{\partial t} = -\nabla \cdot (\bar{v} \bar{P} - \bar{\rho} \bar{Q} \bar{\zeta} + \bar{v}' P' - \bar{\rho}' Q' \bar{\zeta}')'$$

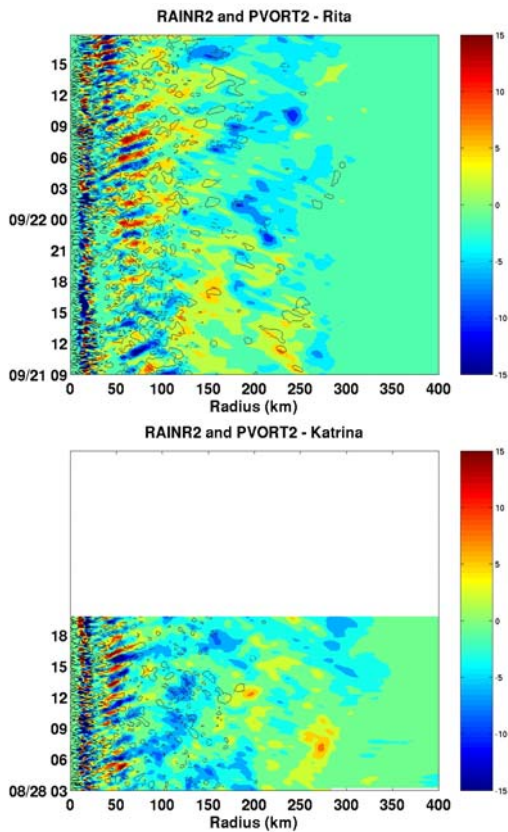


Fig. 2. Radius-time plots of wavenumber 2 rain rate (colored) and PV (contoured).

where P is PV, \vec{v} the three-dimensional wind vector, ρ density, Q diabatic heating rate ($\frac{d\theta}{dt}$), $\vec{\zeta}$ the three-dimensional vorticity vector. The left hand side of the equation is the local rate of change of azimuthal mean PV. The right hand side includes the contributions of flux divergence of mean PV, mean diabatic heating, flux divergence of eddy PV, and the eddy diabatic heating terms.

Frictional effects are small compared to the terms above (Wang, 2002) and have been omitted in this analysis. The vast majority of the PV generation within a tropical cyclone takes place at lower levels in the eyewall (Fig. 3, panel a). Here the positive vertical heating gradient is aligned with the vertical vorticity component and both are large in the eyewall. It should be noted that due to the strong horizontal/vertical shear in the inner core region the horizontal vorticity components were found to be almost as big in magnitude as the vertical component ($\sim 10^{-3} \text{ s}^{-3}$)

and cannot be neglected when examining the PV tendency.

The PV generated below the level of maximum heating is partially depleted above this level since the heating gradient reverses sign above the level of maximum heating at ca. 500 mb (not shown). However, at the uppermost levels of the troposphere the vorticity changes sign as well (anticyclonic outflow), but usually the anticyclonic turning takes place some distance from the regions of strong heating and is weak compared to positive vorticity at lower levels. As the figure shows, an equal amount of heating-generated PV is advected upward (PV flux divergence) with the mean rising motion in the eyewall so that the local derivative of PV is roughly zero. Katrina's eyewall is much more efficient in generating heating-related PV with values of 40 PVU/h compared to Rita (20 PVU/h).

The striking PV depletion near the inner edge of the eyewall is due to diabatic cooling in the downdrafts proposed by Willoughby (1998) and is in Rita almost as big in magnitude as the generation in the eyewall when integrated over a longer period. In the eye at 10 km radius a secondary peak in diabatic heating related PV generation can be seen. We hypothesize that this peak is due to vigorous buoyant updrafts which do not follow the slantwise neutrally-symmetric trajectories of air rising in the eyewall cloud.

Of particular interest are the eddy contributions since our main goal is to determine eddy influence on intensity changes of the whole storm. In general it can be inferred that the eddy contributions are smaller than the mean near the eyewall (Fig. 3, panels a and b). It is evident that eddies (VRW) convey PV from the eyewall into the eye as well as outward. The way this process is accomplished is twofold, through eddy flux divergence and eddy diabatic heating. It turned out that in Katrina eddies are efficient in transporting PV outward whereas eye-ward the eddy heating contribution is larger (Fig. 3, panel b). Rita in contrast has a greater eddy flux convergence into the eye and eddy heating contributions on either side of the eyewall of equal size. This is consistent with the finding that outward propagating VRW are more active in Katrina and so constitute PV redistribution outside the eyewall to a greater extent.

As far as the outer regions are concerned, the eddy terms become major

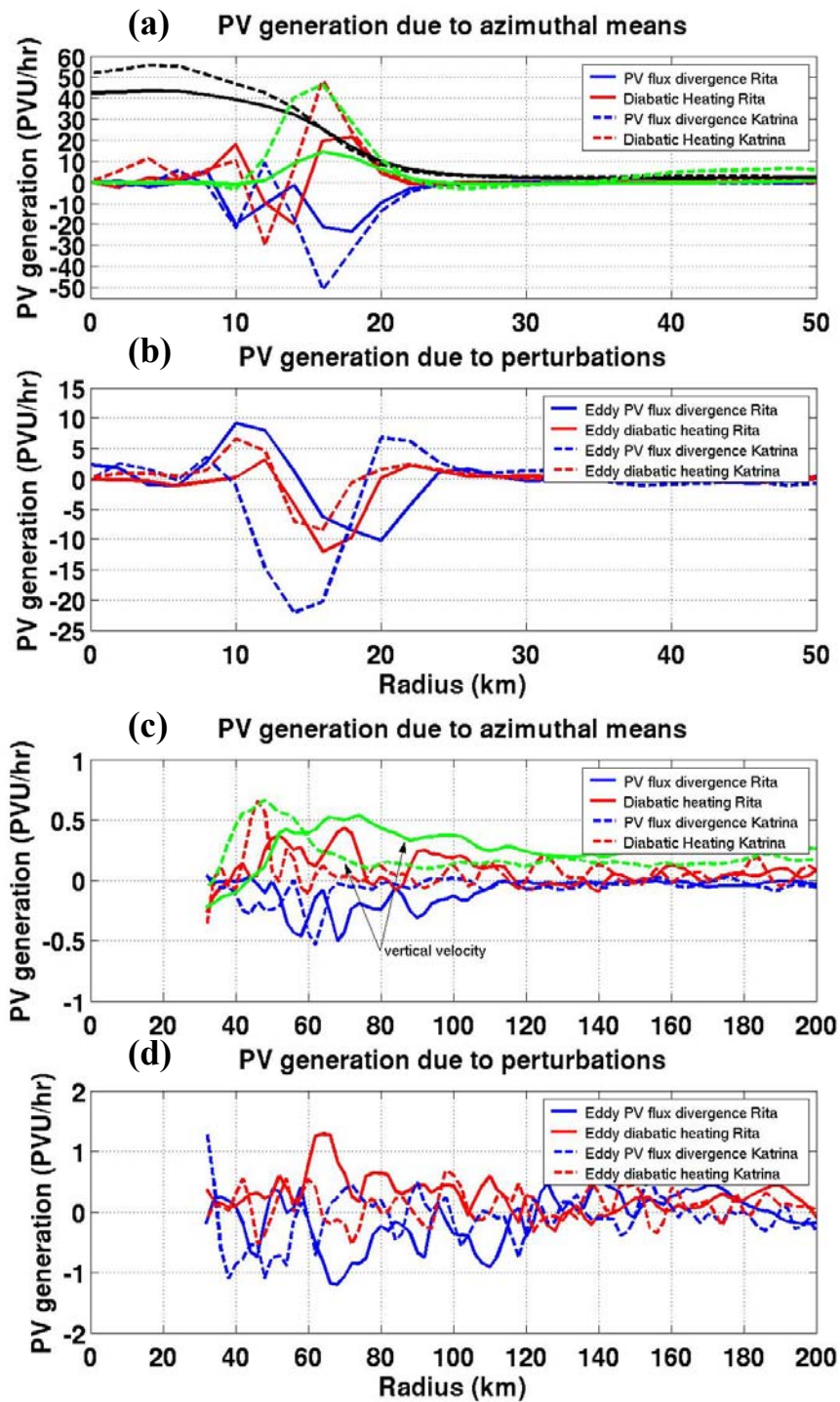


Fig. 3. PV generation/depletion in PVU h^{-1} . Upper two panels highlighting eyewall region, lower two panels provide an enhanced view of the region between 20 and 200 km. Green lines denotes vertical velocity, black lines azimuthally averaged PV; solid Rita, dashed Katrina.

contributors of the PV rate of change because axisymmetry decreases farther from the center and thus the eddy parts are larger in comparison to the mean. PV gains between 60-120 km radius in Rita due to eddy diabatic heating are twice as big as in Katrina and coincide well with the observed secondary wind and PV maximum, as can be inferred from the close-up plots (radius 40-200 km, panels c and d). Due to the high circularity of the rainband, convective generated PV also projects onto the mean. One can see that between 50 and 110 km Rita has positive mean generation rates whereas Katrina's are close to zero beyond 60 km. Katrina's transient rainbands (40-60 km, indicated by the peak in vertical velocity, dashed green line) do have a positive mean rate (Fig. 3, panel c) but not so in the eddy panel. This region of PV generation in Katrina is quite narrow and so overall PV generation in Rita's outer region is much larger.

To further examine the difference in convectively induced PV, Katrina's PV tendencies were subtracted from Rita's (Fig. 4). Clearly evident is Rita's excess between 50-120 km. In particular the eddy contributions play a major role with excess PV generation values near 1.5 PVU h^{-1} , close to the absolute magnitude. This big difference between the storms can certainly be ascribed to the different rainband patterns. Katrina's transient rainbands closer to the storm center do not accumulate PV. While there is little PV generation due to eddy diabatic heating the eddy flux divergence term is comparatively large.

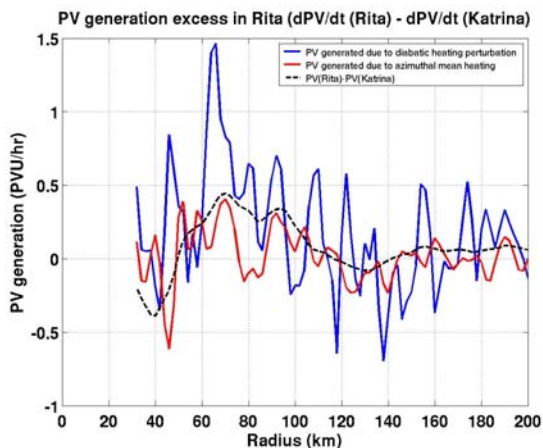


Fig. 4. PV generation difference (Rita minus Katrina). Blue denotes PV generation due to eddy heating perturbations, red indicates PV generation due to azimuthal mean heating. Black dashed line is azimuthal mean PV difference.

This can be explained by the activity of propagating VRW. Rita's outer rainband region features many eddies inducing heating generated PV which lead more effectively to an increase in PV and thus contribute to the secondary maximum of PV.

5. WAVE-MEAN FLOW INTERACTION

According to theory, VRW originating from the eyewall derive their kinetic energy from the mean flow. They convey this momentum away from their excitation region and deposit it in the eye and at the stagnation radius where it accelerates the mean flow.

MK (1997) proposed that this mechanism may lead to the formation of secondary wind maxima and subsequently eyewall replacement cycles. We calculated the eddy momentum flux divergence according to

$$(2) \quad \frac{\partial \bar{v}}{\partial t} = -\frac{\partial}{r^2 \partial r} (\overline{r^2 u'v'})$$

where u is radial velocity, v tangential velocity and r radius. Primes denote perturbation components, bars indicate azimuthal means.

The results in Katrina partly support the hypothesis and indicate a deceleration of the mean flow at the RMW by more than 5 m s^{-1} per hour (Fig. 5, upper panel). The eddies convey momentum primarily inward and accelerate the flow in the eye. However, in contrast to simple numerical model simulations (MK, 1997) it is more difficult to discern the acceleration slightly inside the stagnation radius. A minor increase (0.13 m s^{-1} per hour) can be detected in Katrina at $\sim 60 \text{ km}$. A larger second positive contribution is located between 80 and 90 km which might also be due to VRW since the stagnation radius cannot be defined strictly at a certain fixed radius. Even farther away from the center the sign of the EMFD is alternating irregularly with a positive peak at about 180 km. These quantitative results show that wave-mean flow interaction implications outside the eyewall due to momentum transport are of minor importance and are unlikely to be the source for secondary wind maxima because of their negligible magnitude.

Rita in turn exhibits a very different, almost reverse pattern. The waves actually intensify the mean wind close to the RMW and decelerate it in the eye and outside the RMW in contrast to the theory. Furthermore, between 40 and 120 km from the center the EMFD has 4

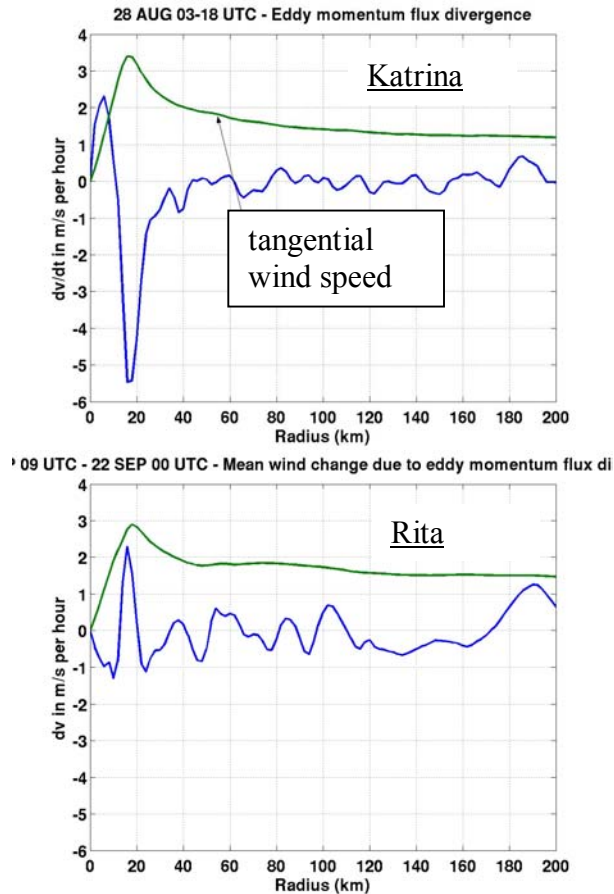


Fig. 5. Acceleration of mean tangential flow due to eddy momentum flux divergence. Upper panel Katrina, lower panel Rita. Green line denotes azimuthally averaged tangential wind.

distinct maxima and minima where the flow is being accelerated/decelerated by ca. 0.5 m s^{-1} per hour. These velocity changes are probably not due to VRW since in this period wave activity was very low.

6. CONCLUDING REMARKS

Both Rita and Katrina were first analyzed in terms of VRW. Katrina's inner core dynamic features are active whereas Rita does not show significant VRW activity before the beginning of the eyewall replacement cycle. Thus VRW influence on the formation of secondary wind maxima is not of great importance at least from a momentum transport perspective as was shown by the eddy momentum flux analysis. The PV budget examination revealed that most of the PV in a tropical cyclone is generated in the mean eyewall convection. In Katrina eddy components for $r > 25 \text{ km}$ are much smaller than for Rita and do not project onto the mean,

except for transient features between 40-60 km. Katrina features PV generation rates in the eyewall twice as large as Rita whereas Rita's outer PV generation rates (especially the eddy parts) exceed Katrina's. This seems to be necessary for the formation of a secondary PV maximum because without Rita's production of PV at large radii it would not have developed a ring of elevated PV which is closely related to the secondary wind maximum that can develop into a secondary eyewall.

Eddy-mean flow interaction showed that VRW increase the velocity in the eye, the tendency outside the eyewall is not very clear. In Rita however, the tendency is reversed with acceleration at the RMW.

Acknowledgments

We wish to thank Dr. Wei Zhao for his assistance in the model simulations and Derek Ortt for helpful discussions during the course of this study.

This research is supported by the NSF RAINEX research grant ATM- 0432717.

REFERENCES

- Chen, Y. and M. K. Yau, 2001: Spiral Bands in a Simulated Hurricane. Part I: Vortex Rossby Wave Verification, *J. Atmos. Sci.*, **58**, 2128-2144
- , and -, 2003: Spiral Bands in a Simulated Hurricane. Part II: Wave Activity Diagnostics. *J. Atmos. Sci.*, **60**, 1239-1256
- and -, 2003: Asymmetric Structures in a Simulated Landfalling Hurricane. *J. Atmos. Sci.*, **60**, 2294-2312
- Kossin, J. P. et al, 2000: Unstable Interactions between a Hurricane's Primary Eyewall and a Secondary Ring of Enhanced Vorticity. *J. Atmos. Sci.*, **57**, 3893-3917
- Montgomery, M. T. and R. J. Kallenbach, 1997: A Theory for vortex Rossby-waves and its application to spiral bands and intensity changes in hurricanes. *Q.J.R. Meteorol. Soc.*, **123**, 435-465

Ortt, D., and S. S. Chen, 2006: Rainbands and secondary eyewall formation as observed in RAINEX. *27th Conf. on Hurricanes and Tropical Meteorology*. 23-27 April 2006, Monterey, CA, Amer. Meteor. Soc. 12A.5.

Ortt, D., 2007: Effects of environmental water vapor on tropical cyclone structure and intensity. Master's Thesis, University of Miami 91pp.

Reasor, P. D. et al., 2000: Low-Wavenumber Structure and Evolution of the Hurricane Inner Core Observed by Airborne Dual-Doppler Radar., *Mon. Weather Rev.*, **128**, 1653-1679

Schubert, W. H. et al, 1999: Polygonal Eyewalls, Asymmetric Eye Contraction, and Potential Vorticity Mixing in Hurricanes. *J. Atmos. Sci.*, **56**, 1197-1223

Wang, Y., 2002: Vortex Rossby Waves in a Numerically Simulated Tropical Cyclone. Part I: Overall Structure, Potential Vorticity, and Kinetic Energy Budgets. *J. Atmos. Sci.*, **59**, 1213-1238

-, 2002: Vortex Rossby Waves in a Numerically Simulated Tropical Cyclone. Part II: The Role in Tropical Cyclone Structure and Intensity Changes. *J. Atmos. Sci.*, **59**, 1239-1262

Willoughby, H. E. et al, 1982: Concentric Eye Walls, Secondary Wind Maxima, and The Evolution of the Hurricane Vortex. *J. Atmos. Sci.*, **39**, 395-411

-, et al, 1984: Stationary and Moving Convective Bands in Hurricanes. *J. Atmos. Sci.*, **41**, 3189-3211

-, 1998: Tropical Cyclone Eye Thermodynamics. *Mon. Weather Rev.*, **126**, 3053-3067

Wu, L. and Wang, B., 2000: A Potential Vorticity Tendency Diagnostic Approach for Tropical Cyclone Motion. *Mon. Weather Rev.*, **128**, 1899-1911